Mathematical Model for Aerodynamic Interaction of High-Speed Passenger and Freight Trains on Adjacent Tracks. Part I: Preliminary Conclusions on Problem Formulation and Solution Approach

Marufdjan Rasulov[1,2], Masud Masharipov[1,2], Ramazon Bozorov[1,2] and Lazokat Kodirova[1,2]
[1]*Tashkent State Transport University, Temiryolchilar Str. 1, 100167 Tashkent, Uzbekistan*
[2]*University of Diyala, 32009 Baqubah, Diyala, Iraq*
tashiit_rektorat@mail.ru, masudcha@mail.ru, ramazon-bozorov@mail.ru, lazokaticegirl@gmail.com

Keywords: High Speed, Aerodynamics, Safe Crossing, Freight Train, Standard, Air Flow, Anemometer, Kinematic Viscosity.

Abstract: The article highlights the theoretical formulation of the problem of studying the issues of mutual aerodynamic influence that affects the organization of safe crossing of high-speed passenger and freight trains when they move along adjacent railway tracks. The issue of operating freight trains without unnecessary stops in railroad sections with mixed traffic of different types of trains acquires urgent importance. With the help of the Navier-Stokes equation, which is primary in hydrogasdynamics for the study of aerodynamic effects, the nature of air flows that occur during the movement of trains of different categories has been studied. The problem of modeling the dynamics of changes in aerodynamic pressure impulses with respect to time and coordinate is described in detail. Preliminary conclusions on the determination of aerodynamic pressure showed that all speeds of freight and high-speed passenger trains used on the correct sections of Uzbekistan railways shouldn't exceed the calculated total pressure, to ensure the safety of train movement.

1 INTRODUCTION

When evaluating the aerodynamic forces, pressure, and safe distance experienced by passengers standing on adjacent tracks within a moving train or on a platform beside the tracks, the pressure (Pa) specified in safety standards, the distance of the object from the centerline of the tracks S (in meters), and the train speed V (in km/h) are expressed as a function. Solving this problem will enhance the capacity of the train section while ensuring traffic safety, thereby addressing issues related to the passage of freight trains in high-speed passenger train sections [1], [2].

The determination of the aforementioned parameters requires consideration of multiple factors. Specifically, the air surrounding the train is treated as an incompressible turbulent flow, and the Navier-Stokes equation is solved. The general form of the Navier-Stokes equation is as follows (1) in Appendix [1]-[2], [12].

Here u_x , u_y , u_z - projections of the velocity vector on the x, y, z axes; p - pressure; ρ - density; T - temperature; μ - is the coefficient of dynamic viscosity of air.

The continuity (2), derived from the principles of state and mass conservation, is obtained as follows:

$$\frac{\partial \rho}{\partial t}+\frac{\partial(\rho u_x)}{\partial x}+\frac{\partial(\rho u_y)}{\partial y}+\frac{\partial(\rho u_z)}{\partial z}=0 \quad (2)$$

If we consider this process in the $\{x, y\}$ plane and for an ideal gas, ($u_x >> u_z, u_y$, $\rho = const.$) The Euler equation in a particular case has the following (3) in Appendix [1]-[2], [12].

The relationship between the boundary layer width and the ratio of velocities in the incompressible turbulent airflow, as a function of the x coordinate (distance to the head of the train), was determined using the power law [1], [2]:

$$\begin{cases} \frac{u_x}{U} = \sqrt[7]{\frac{y}{\delta}} \\ \delta(x)_{turbulent} = 0{,}37 \cdot \sqrt[5]{\frac{\nu \cdot x^4}{U}} \\ \delta(x)_{laminar} \approx 5 \cdot \sqrt{\frac{\nu \cdot x}{U}} \end{cases} \quad (4)$$

Here u_x - the projection of the velocity vector in the direction of the *ox* axis is expressed in meters per second (m/s); U - train speed, m/s; y - The distance from the side surface of the train in the direction of the *oy* axis is expressed in meters (m); δ - boundary layer width of incompressible turbulent air flow, m; x - distance to the head of the train, m; ν - coefficient of kinematic viscosity of air at a given temperature, m^2/s;

Figures 1-2 illustrates the relationship between the width of the boundary layer of the air flow $\delta(x)$) and the speed of the air flow on the coordinate axis ($U \leq 250\ km/coam$).

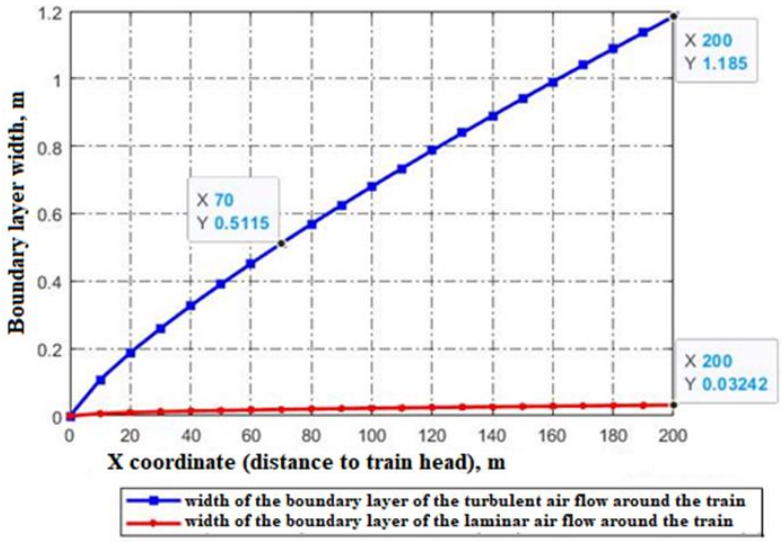

Figure 1: A plot of airflow boundary layer width versus the x coordinate (distance to the head of the train).

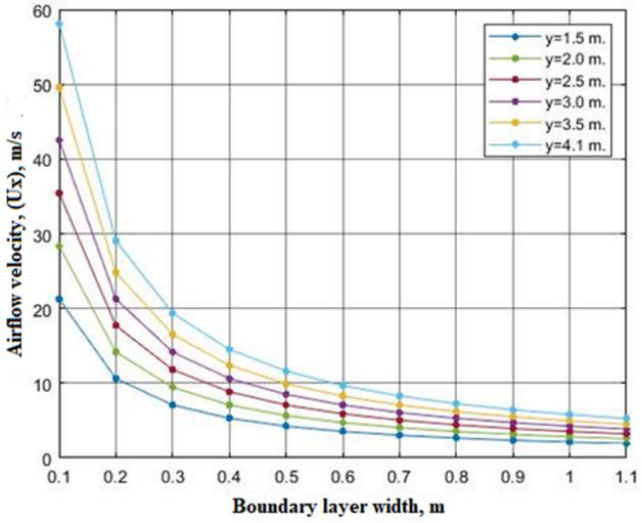

Figure 2: A graph of the relation of air flow speed to the width of the boundary layer.

2 MATERIALS AND METHODOLOGY

From the presented graphs, it is evident that both the width of the boundary layer and the velocity of the airflow exhibit a continuous and smooth variation. When observing the train's movement in the XOZ plane, the simplified vector Navier-Stokes equation can be employed, utilizing the "Reynolds-averaged Navier-Stokes (RANS) method." The specific form of this equation is as follows (5) in Appendix [1]-[2].

It is possible to simplify the above expressions depending on the characteristic indicators, in particular (6) in Appendix.

In a similar manner, the characteristic parameters of the second part will take on the following (7) in Appendix.

Based on (6) and (7), expression (5) can be simplified as follows:

$$\begin{cases} \bar{u}_x \frac{\partial \bar{u}_x}{\partial x} + \bar{u}_z \frac{\partial \bar{u}_x}{\partial z} + \frac{1}{\rho}\frac{\partial \bar{p}}{\partial x} = \nu \cdot \frac{\partial^2 \bar{u}_x}{\partial x^2} - \frac{\partial \bar{u}_x' \bar{u}_z'}{\partial z} \\ \frac{1}{\rho}\frac{\partial \bar{p}}{\partial z} = 0 \\ \frac{\partial \bar{u}_x}{\partial x} + \frac{\partial \bar{u}_z}{\partial z} = 0 \end{cases} \quad (8)$$

Based on (8), it is possible to determine the function describing the dependence of the velocity components on the width of the boundary layer and the Reynolds number, specifically for the conditions where $u_x >> u_z, u_y$.

$$\frac{u_x}{U} = \frac{1}{0{,}41} \cdot \ln(\frac{z}{z_o}) \quad \text{or}$$

$$u^+ = \frac{1}{0{,}41} \cdot \ln(\frac{z \cdot U}{\nu}) + K = \frac{1}{0{,}41} \cdot \ln(z^+) + K$$

The obtained results in both planes demonstrate a systematic variation in the velocity components.

To ensure the reliability of the theoretical calculations, it is crucial to compare them with the results of experimental tests conducted by various researchers [3]-[12]. These experiments employed specialized anemometric instruments equipped with a Pitot tube (as shown in Figure 3) to measure residual differential pressures, dynamic pressures, and flow velocity.

The aerodynamic characteristics and mutual interaction of high-speed passenger and freight trains differ significantly from the interaction between two high-speed passenger trains. Extensive scientific research conducted by English, French, and Polish scientists [1], [3], 5], [7] has revealed a pronounced aerodynamic effect when high-speed trains move in opposite directions. The aerodynamic effects of high-speed passenger trains at intersections were compared in three different scenarios [13]:

- The observing train is moving at a speed lower than the passing train;
- The velocities of the observer and the passing train are equal;
- The following train is stationary.

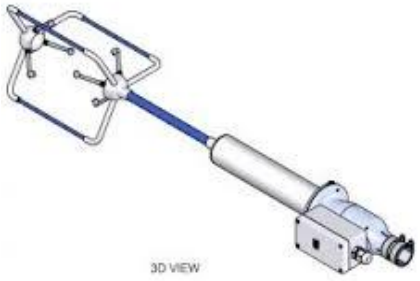

(a)

(b)

Figure 3: Equipment used in experimental work. a) 3D-Axis Ultrasonic Anemometr, b) PCE-HVAC Model 2 Pitot Tube Anemometer.

Experimental results indicated that the highest aerodynamic pressure was observed in case 3, as shown in Table 1. Furthermore, it was observed that the magnitude of the residual pressure difference on the windows of high-speed trains moving in opposite directions at different speeds (160/140 km/h) was lower than the standard value (of 1800 Pa).

Experimental results [5] showed that the maximum pressure created when two trains cross has the following values.

Figure 4 quantifies this relationship, showing how aerodynamic pressure (Pa) escalates with increasing train speeds at varying horizontal distances between track centers (3.8–4.5 m). Figure 4 visualizes the pressure trends from Table 1, highlighting the exponential growth with speed.

Table 2 complements these findings by quantifying the maximum aerodynamic pressure exerted on the sidewall of the ET2M train during crossings with the Sapsan high-speed train under varying speed conditions

It is crucial to investigate the aerodynamic characteristics of airflow around trains to ensure safe crossings when encountering oncoming trains. Drawing upon scientific studies [6], [7], [9], [14] the model representing the airflow nature at train intersections can be expressed as follows in Figure 5.

Table 1: The aerodynamic pressure values obtained from the experimental test results.

Train speed, km/h	Aerodynamic pressure, Pa			
	Horizontal distance between road axes, m			
	3,8 (m)	4,0 (m)	4,2 (m)	4,5 (m)
160	328,3	282,0	245,2	202,8
180	415,5	356,8	310,3	256,6
200	512,9	440,6	383,1	316,8
220	-	533,1	463,5	383,3
240	-	634,4	551,6	456,2
250	-	688,4	598,6	495,0
260	-	-	647,4	535,4
280	-	-	750,8	620,9
300	-	-	861,9	712,8
320	-	-	-	811,0
340	-	-	-	915,6
350	-	-	-	970,2

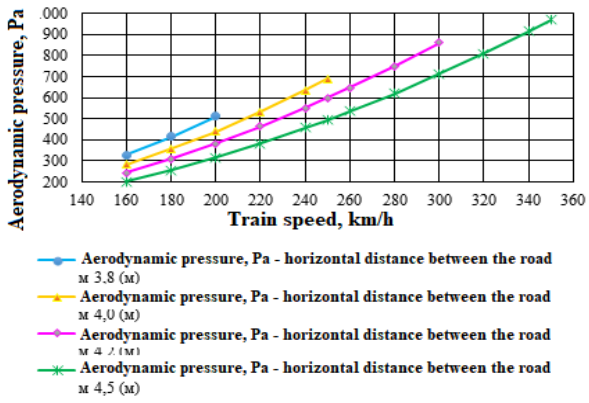

Figure 4: Value of aerodynamic pressure based on experimental results

Table 2: The maximum pressure exerted on the side wall of the car when trains are crossing.

Speed of trains at intersection, km/h		The maximum aerodynamic pressure on the sidewall of the ET2M train, Pa
Sapsan	ET2M	
160	0 (stayed on the neighboring road)	230
200	0	325
250	0	525
250	60	580
250	100	610
250	120	650
275	0	600
275	120	780

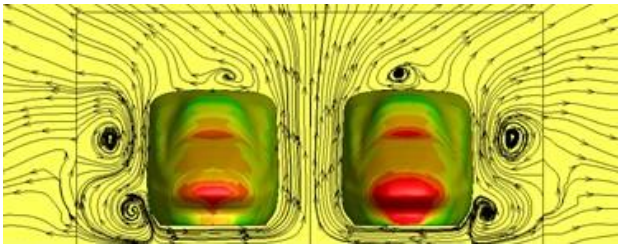

Figure 5: The nature of the air flow around oncoming trains.

In the context of the current study, the analysis focuses on a specific scenario involving a freight train. The freight train under consideration has a total length of 815 meters and a gross weight of 1392 tons. This freight train is composed of an electric locomotive called "Afrosiyob" with a gross weight of 310 tons, which is accompanied by 11 cars with a combined length of 183 meters. Additionally, two locomotives are also present in this configuration. The objective is to examine the safety conditions at the intersection, as depicted in Figure 6.

Based on extensive scientific research conducted by various scholars [3]-[5], [9], the characteristics of airflow and air pressure during the crossing of two trains can be summarized as depicted in Figure 7. The safe crossing of trains and their stability [15], along with the study of the impact of airflow on loads in open rolling stock resulting from their interaction with high-speed trains, is a critical and pressing issue. In this regard, the airflow between high-speed passenger and freight trains is considered as an incompressible turbulent air flow [1].

To ensure train stability, it is crucial to take into account the merging and reinforcement of the air

currents formed around the two trains. In this scenario, the primary transverse aerodynamic force is generated at the head of the rolling stock, while the force between the cars is relatively lower [1], [3], [11]. The dominant aerodynamic force, which significantly affects train stability, acts in the transverse direction along the axis of the train. This force is attributed to the organization of turbulent air flows in that particular direction. Experimental tests [4], [7], [9] confirm that the flow speed around trains decreases gradually and follows a certain pattern as it moves away from the train.

Considering the above observations, the overall air flow velocity can be expressed in the following manner, taking into account the principle that the speed of the flow around trains decreases gradually in relation to the speed of the ambient air flow at points distanced from the train.

$$\vartheta = V_n\left[1-\left(\frac{y}{\delta}\right)^{1/n}\right] \qquad \delta = a\cdot X^{m}. \quad (9)$$

Here, ϑ - air flow speed around the train, m/s; V_n - speed of a high-speed passenger train, m/s; y - transverse distance from the vehicle body to the observation point, m; n, m, a - fixed coefficients depending on the composition and type of train; X - horizontal distance to the front of the train, m

According to the European standard "EN 14067 Railway application - Aerodynamics - Chapter 4" [3]-[4], the calculation of the speed components of a turbulent air stream formed around a circular train is determined as follows (10):

$$C_{vi} = \vartheta_i / V_п;\ C_{vx} = \vartheta / V_п;\ C_{uy} = u / V_п;\ C_{wz} = w / V_п \quad (10)$$

Here ϑ, u, w - velocity components of the air flow formed around the train, m/s; V_n - speed of a high-speed passenger train, m/s; C_{vx}, C_{uy}, C_{wz} - constant speed coefficients depending on the composition and type of train $0{,}17 \le C_{vx} \le 0{,}4$; $C_{uy} \le 0{,}1$; $C_{wz} \le 0{,}1$; $C_{vx}(freighttrain) \le 0{,}57$.(freight train).

Based on Figure 7 and scientific research, it can be observed that pressure pulses exhibit varying patterns at different points, dependent on time and coordinates. Therefore, a model was developed to simulate the aerodynamic pressure impulses, as depicted in Figure 8.

The graph illustrates that the pressure exhibits a linear trend in zones 0, 4, 8, n-1, and a sinusoidal pattern in zones 1, 2, 3-5, 6, 7-9, 10, 11-n-4, n-3, n-2, but in reverse order. Consequently, the variation in coordinates and pressure impulses is expressed in the following manner:

$$\begin{cases} x_1 - x_0 = (\vartheta_1 + \vartheta_2)\cdot(t_1 - t_0) \\ x_2 - x_1 = (\vartheta_1 + \vartheta_2)\cdot(t_2 - t_1) \\ x_3 - x_2 = (\vartheta_1 + \vartheta_2)\cdot(t_3 - t_2) \\ \vdots \\ x_n - x_{n-1} = (\vartheta_1 + \vartheta_2)\cdot(t_n - t_{n-1}) \end{cases} \quad (11)$$

In a linear order, the pressure values in the change zones were determined by expression (12) in Appendix.

The pressure value was determined using expression (13) in Appendix by changing the zones in a sinusoidal order.

The magnitude of the aerodynamic force acting on each of them is determined by integration. From expressions (12), (13) it can be seen that the peak aerodynamic pressure corresponds to zones 1, 2, 3. Also, based on the results of the above scientific research and European standards, assuming the maximum value of aerodynamic pressure corresponding to zones 1, 2, 3, affecting the stability of trains, proportional to the square of the speed of the train, the pressure of a high-speed passenger train on a freight train in the transverse direction along the axis of *oy* and *oz* (14) in Appendix was determined by the expression [12].

Here k_1 – coefficient of influence depending on the geometric structure of the train ($k_1^{freight} \approx 1$; $k_1^{passenger} \approx 0{,}53$; $k_1^{high-speed} \approx 0{,}43$); y – distance between axes of adjacent roads ($y = 4{,}1\ м$), m; A_1 – width of the investigated object or rolling stock (width of a locomotive or carriage of a high-speed passenger train, $A_1 = 2{,}96\ m$), m; A_2 – width of the object or rolling stock under study (width of a locomotive or wagon of a freight train, $A_2 = 3{,}1\ m$), m; ρ – air density ($\rho \cong 1{,}2041\ kg/m^3$), kg/m^3; ϑ_1, ϑ_2 – speed of high-speed passenger and freight trains ($\vartheta_1^{\max} = 250\ km/h \approx 69{,}44\ m/s$, $\vartheta_2^{\max} = 90\ km/h \approx 25\ m/s$), m/s.

C_{p1} – Coefficient of aerodynamic pressure in the direction of the axes *oy* and *oz*.

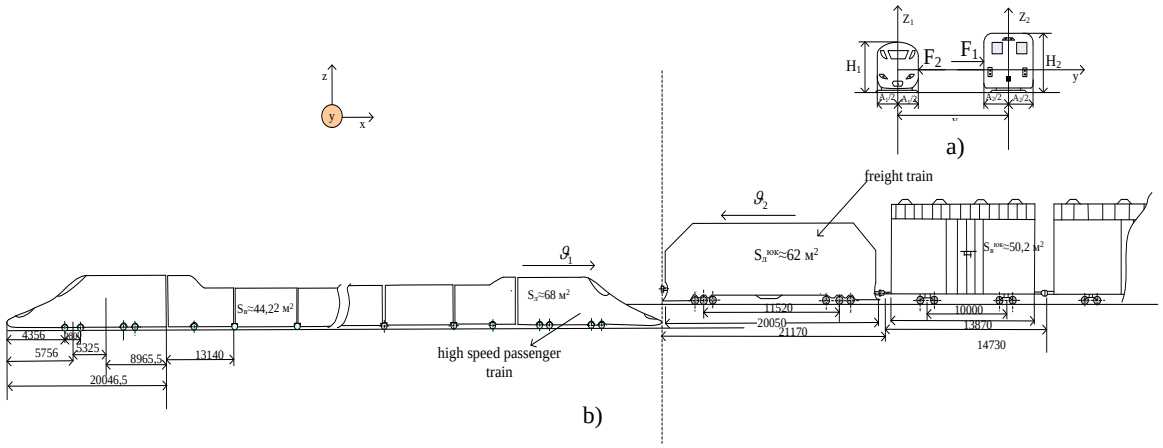

Figure 6: Design diagram of the intersection of the Afrosiab high-speed electric train and a freight train on neighboring tracks: a) section, b) side view.

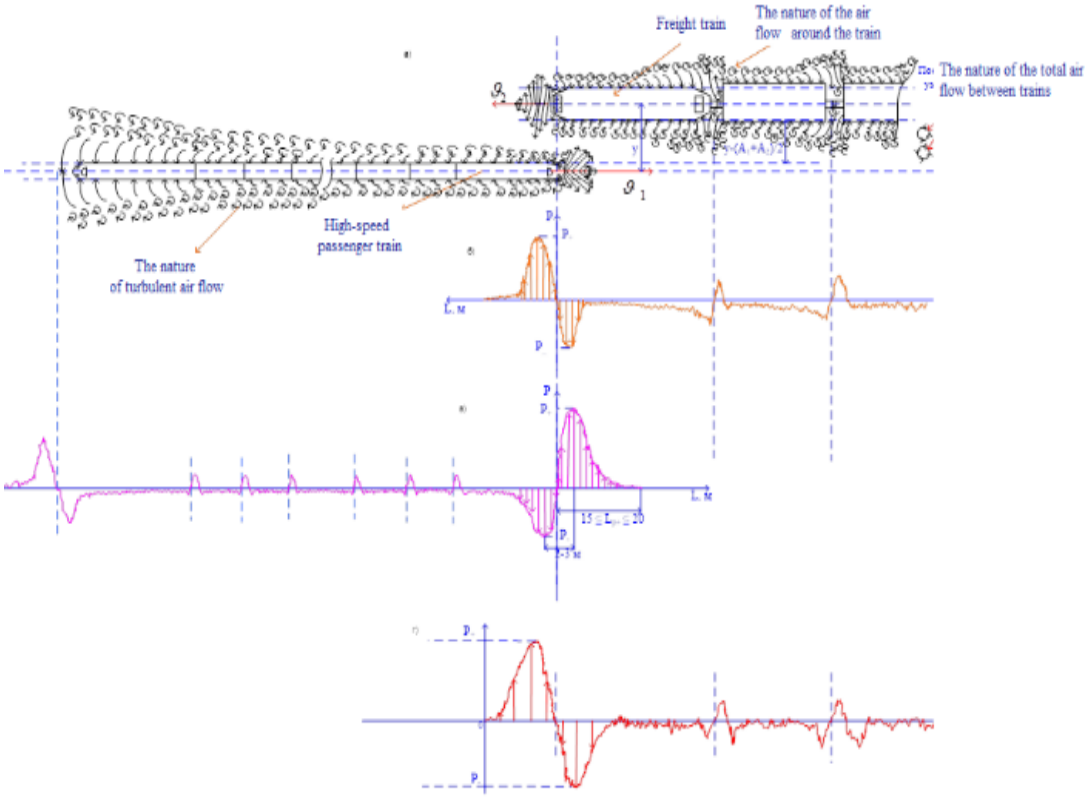

Figure 7: Calculation diagram of the intersection of the Afrosiab high-speed electric train and a freight train on adjacent tracks: a) - top view, b), c), d) - freight, high-speed and the nature of the dynamics of changes in aerodynamic pressure at their intersection.

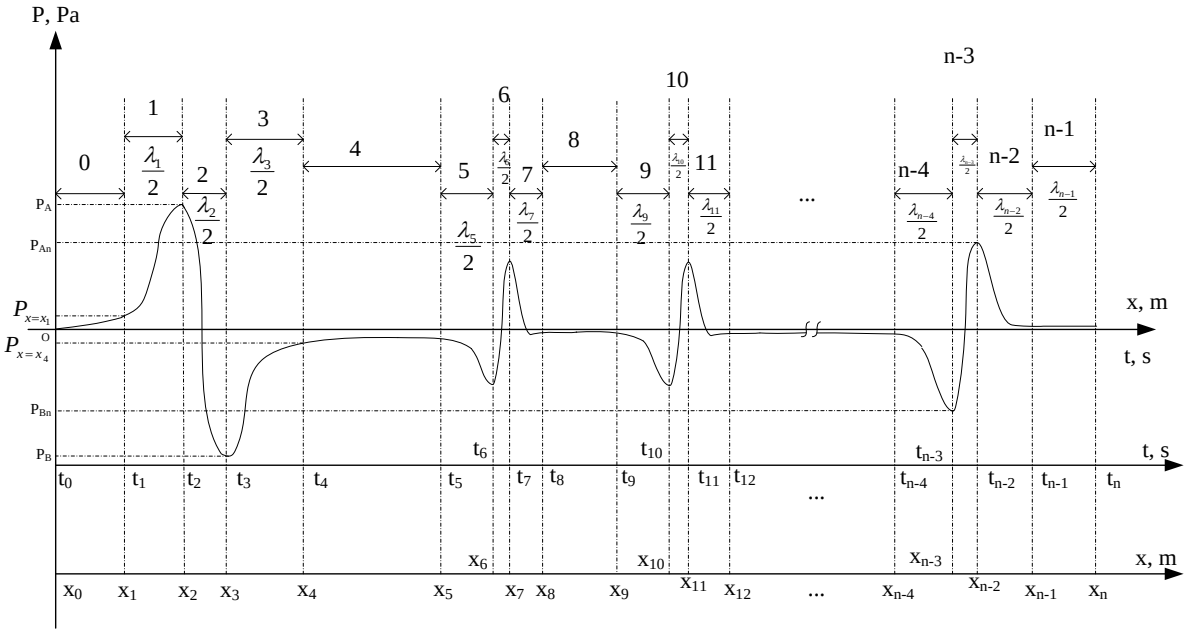

Figure 8: The law of change of the impulse of aerodynamic pressure depending on time and coordinates.

Since in our case $\vartheta_{max} = \vartheta_1 = 250\ {}^{km}/_{h} \approx 69{,}44\ {}^{m}/_{s}$, the maximum number $M = {}^{\vartheta_{max}}/_{c} \approx 0{,}21$ and the Reynolds number $4{,}5\cdot10^{8} \le \mathrm{Re} = {}^{\vartheta_1 \cdot L_п}/_{\nu} \le 7{,}1\cdot10^{8}$ (+20 ^{0}C $\nu = 1{,}81\cdot10^{-5}\ {}^{m^2}/_{s}$) were taken, and the process under consideration was studied as incompressible air in a stationary state. Similarly, the aerodynamic effect of a freight train on a passenger train was expressed as follows:

$$\begin{cases} \Delta P_{2y} = k_1^{freight} \cdot C_{p2y} \cdot \rho \cdot \dfrac{\vartheta_2{}^2}{2 \cdot 3,6^2} \\ C_{p2y} = \dfrac{8}{\left(y - \dfrac{A_1}{2} + 2{,}10\right)^2} \\ \Delta P_{2z} = k_1^{freight} \cdot C_{p2z} \cdot \rho \cdot \dfrac{\vartheta_2{}^2}{2 \cdot 3,6^2} \\ C_{p2z} = \dfrac{8{,}5}{(z-1{,}9)^2} + 0{,}1 \end{cases}$$

In a comprehensive analysis, the peak pressure occurring in the transverse direction as a consequence of train intersection and negatively impacting their stability was determined by applying the principle of superposition, considering the combined effect of pressure values and the compressive force resulting from the addition of their air flow velocities in the most unfavorable scenario. Furthermore, in accordance with the technical specifications for load fastening and enhancement, an average external wind pressure of 50 kgs/m^2 ≅ 500 Pa was assumed.

$$\Delta P_y^{\text{total}} = \sum_{i=1}^{n} \Delta P_{iy} = \Delta P_{1y} + \Delta P_{2y} + \cdots + \Delta P_{ny}$$

$$\begin{cases} F_{y1} = \Delta P_y^{\text{total}} \cdot S_2 \\ F_{y2} = \Delta P_y^{\text{total}} \cdot S_1 \end{cases}$$

3 RESULT AND DISCUSSION

As a result of determining the resulting aerodynamic and total pressure using the MATLAB program, the following graphs were constructed (Figure 9 and Figure 10).

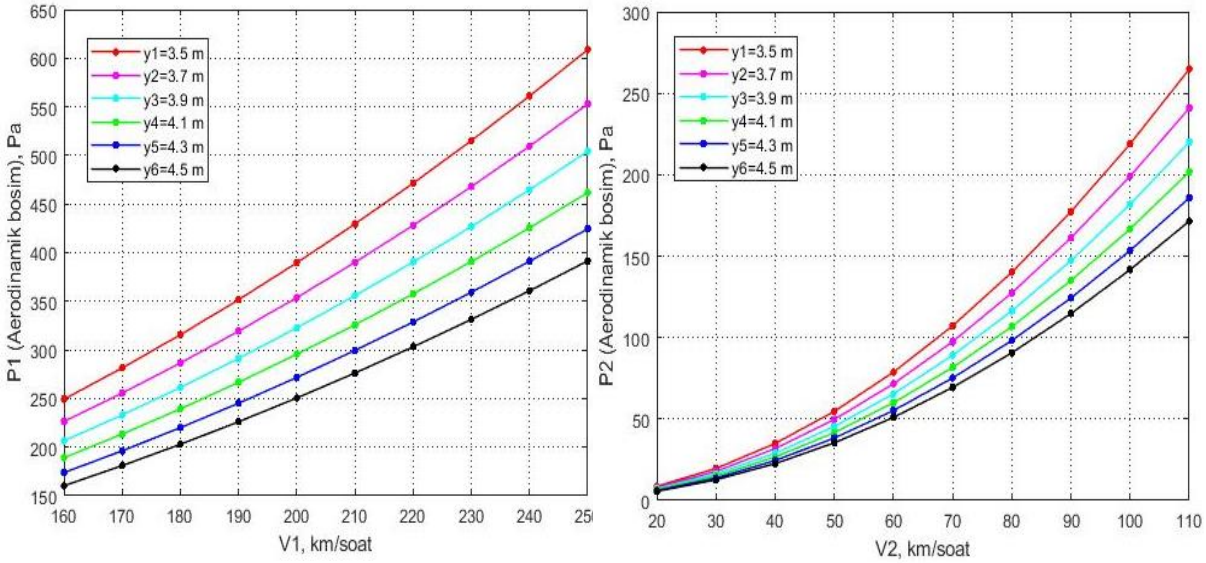

Figure 9: The value of the aerodynamic pressure of high-speed (left) and freight trains (right).

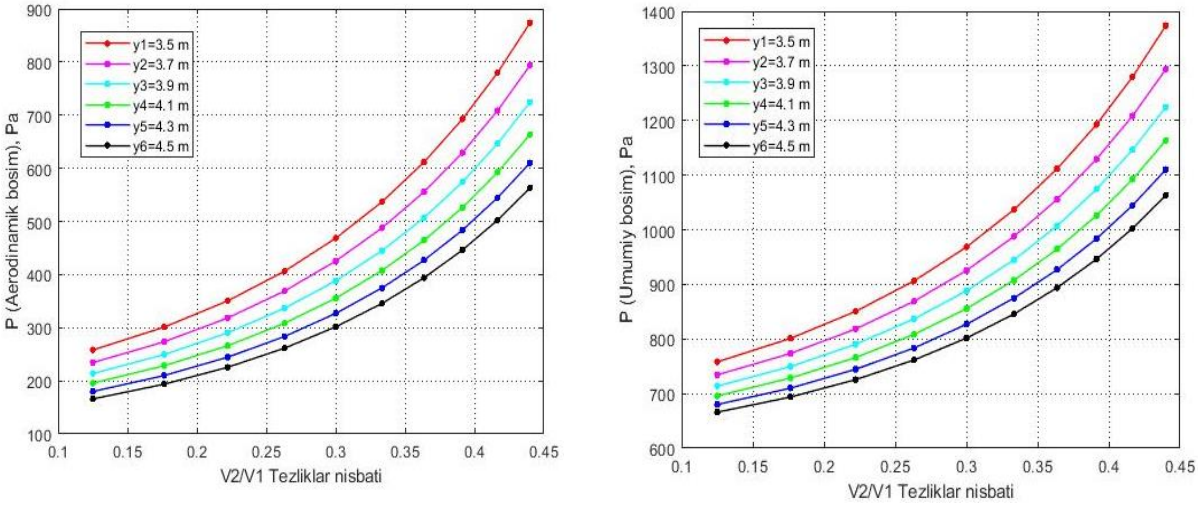

Figure 10: The value of the aerodynamic pressure created between trains (left) and the total pressure (right) taking into account the influence of external wind.

4 CONCLUSIONS

The issue of operating freight trains without unnecessary stops in railroad sections with mixed traffic of different types of trains acquires urgent importance. Based on the analysis of scientific research conducted from this perspective, it was determined that the nature of the air flow around trains during intersection at speeds of up to 250 km/h for passenger trains and up to 100 km/h for freight trains is compressible (M <0,3). The peculiar solutions of the Navier-Stokes equations were also considered in determining the width of the boundary layer of air flow velocity. In order to ensure safe movement during the intersection of trains, the law of change of the aerodynamic pressure impulse occurring between them in a time- and coordinate-dependent manner was modeled; the general aerodynamic pressure that could affect the moving units was determined based on the principle of

superposition and the achieved results were compared with regulatory values.

Based on the proposed mathematical model, the calculated value of the aerodynamic pressure is 628,7 Pa (250/100), and when compared with the results of scientific research [4], the relative error is about, indicating that the accuracy of the engineering calculations is within the standard value of approximately ( ).

The results of the calculations showed that when the distance between the rails is 4,1 meters and the relative speed of movement of freight and high-speed passenger trains is 0,44 (for example, the maximum speed of the freight train is 110 km/h, and the speed of the high-speed passenger train is 250 km/h), the total pressure is 1164 Pa. This amount of total pressure constitutes 64,7% of the value of the calculated pressure (1800 Pa) specified in the "Safety Standards for Railway Transport" NB JT ST 03-98. Therefore, it can be concluded that all speeds of freight and high-speed passenger trains used on the correct sections of Uzbekistan railways do not exceed the calculated total pressure, which ensures the safety of train movement. In the future, detailed studies will be conducted on the aerodynamic forces that arise during the crossing of trains in complex conditions (on curved sections of the railway, in areas with strong wind influence, etc.) based on the mathematical model developed.

REFERENCES

[1] M. X. Rasulov, M. N. Masharipov, and R. S. Bozorov, "Investigation of mutual aerodynamic influence of high-speed passenger and freight trains moving on adjacent tracks," Journal Innotrans, Scientific and nonfiction edition, no. 2 (44), pp. 42, 2022.

[2] GOST 34093-2017, Vagoni passajirskie lokomotivnoy tyagi. Trebovaniya k prochnosti i dinamicheskim kachestvam, M.: Standartinform, 2017, 45 p.

[3] GOST 33211-2014, Vagoni gruzovie. Trebovaniya k prochnosti i dinamicheskim kachestvam, M.: Standartinform, 2016, 54 p.

[4] GOST 33788-2016, Vagoni gruzovie i passajirskie. Metodi ispitaniy na prochnost i dinamicheskie kachestva, M.: Standartinform, 2016, 41 p.

[5] H. H. Saleh, "Interference Mitigation in the Vehicular Communication Network Using MIMO Techniques," Journal of Engineering Science and Technology, vol. 16, no. 2, pp. 1837-1850, 2021.

[6] G. N. Abramovich, Prikladnaya gazovaya dinamika. Ch.1-Ch.2: uchebnoe posobie, M.: Nauka, 1991, 600 p.

[7] L. G. Loysyanskiy, Mexanika jidkosti i gaza: Ucheb. dlya vuzov, 7-e izd., ispr., M.: Drofa, 2003, 840 p.

[8] I. Mishkhal, S. A. A. L. Kareem, H. H. Saleh, A. Alqayyar, I. Hussein, and I. A. Jassim, "Solving Course Timetabling Problem Based on the Edge Coloring Methodology by Using Jedite," in 2019 1st AL-Noor International Conference for Science and Technology (NICST), 2019.

[9] G. Shlixting, Teoriya pogranichnogo sloya, M.: Nauka, 1974, 712 p.

[10] H. H. Saleh, I. Mishkal, and A. A. Hussein, "Enabling Smart Mobility with Connected and Intelligent Vehicles: The E-VANET Framework," in Proceedings of the International Conference on Applied Innovation in IT, vol. 12, no. 2, pp. 9-17, Nov. 2024, [Online]. Available: https://www.icaiit.org/paper.php?paper=12th_ICAIIT_2/1_2

[11] A. Zbieć, "Aerodynamic Phenomena Caused by the Passage of a Train. Part 2: Pressure Influence on Passing Trains," Problemy Kolejnictwa, no. 192, pp. 195-202, Sep. 2021, [Online]. Available: http://dx.doi.org/10.36137/1926E

[12] NB JT ST 03-98, Safety Standards for Railway Transport. Elektropoezda, M.: VNIIJT, 2003, 196 p.

[13] M. Masharipov, M. Rasulov, S. Suyunbayev, N. Adilova, O. Ablyalimov, and A. Lesov, "Valuation of the influence of the basic specific resistance to the movement of freight cars on the energy costs of driving a train," in E3S Web of Conferences, vol. 383, p. 04096, 2023, EDP Sciences.

[14] S. Shukhrat, R. Bozorov, and E. Shermatov, "Kinematic characteristics of the car movement from the top to the calculation point of the marshalling hump," E3S Web of Conferences, vol. 264, p. 05008, 2021, [Online]. Available: https://doi.org/10.1051/e3sconf/202126405008

[15] A. D. Khomonenko and M. M. Khalil, "Quantum computing in controlling railroads," E3S Web of Conferences, vol. 383, p. 01010, 2023.

APPENDIX

The Appendix contains the detailed mathematical expressions used in the study, specifically formulas (1), (3), (5), (6), (7), (12), (13), and (14), which support the aerodynamic modeling and calculations presented in the main text.

$$\begin{cases} \rho \cdot (\frac{\partial u_x}{\partial t} + u_x \frac{\partial u_x}{\partial x} + u_y \frac{\partial u_x}{\partial y} + u_z \frac{\partial u_x}{\partial z}) + \frac{\partial p}{\partial x} = X + \mu(\frac{\partial^2 u_x}{\partial x^2} + \frac{\partial^2 u_x}{\partial y^2} + \frac{\partial^2 u_x}{\partial z^2}) + \rho \cdot g_x \\ \rho \cdot (\frac{\partial u_y}{\partial t} + u_x \frac{\partial u_y}{\partial x} + u_y \frac{\partial u_y}{\partial y} + u_z \frac{\partial u_y}{\partial z}) + \frac{\partial p}{\partial y} = Y + \mu(\frac{\partial^2 u_y}{\partial x^2} + \frac{\partial^2 u_y}{\partial y^2} + \frac{\partial^2 u_y}{\partial z^2}) + \rho \cdot g_y \\ \rho \cdot (\frac{\partial u_z}{\partial t} + u_x \frac{\partial u_z}{\partial x} + u_y \frac{\partial u_z}{\partial y} + u_z \frac{\partial u_z}{\partial z}) + \frac{\partial p}{\partial z} = Z + \mu(\frac{\partial^2 u_z}{\partial x^2} + \frac{\partial^2 u_z}{\partial y^2} + \frac{\partial^2 u_z}{\partial z^2}) + \rho \cdot g_z \end{cases} \quad (1)$$

$$\begin{cases} \frac{\partial \vec{u}_i}{\partial t} + u_x \frac{\partial \vec{u}_i}{\partial x} + u_y \frac{\partial \vec{u}_i}{\partial y} + u_z \frac{\partial \vec{u}_i}{\partial z} = -\frac{1}{\rho} \nabla_i P \ , \ \varepsilon = \frac{\delta}{L} << 1 \ , \ Re = \frac{L \cdot U}{\nu} = \frac{L \cdot U \cdot \rho}{\mu} >> 1 \\ \rho \cdot (\frac{\partial u_x}{\partial t} + u_x \frac{\partial u_x}{\partial x} + u_y \frac{\partial u_x}{\partial y}) = -\frac{\partial p}{\partial x} \\ \rho \cdot (\frac{\partial u_y}{\partial t} + u_x \frac{\partial u_y}{\partial x} + u_y \frac{\partial u_y}{\partial y}) = -\frac{\partial p}{\partial y} \\ \frac{\partial u_x}{\partial x} + \frac{\partial u_y}{\partial y} = 0, \ u_x = \frac{\partial \psi}{\partial y}, u_y = -\frac{\partial \psi}{\partial x} \Rightarrow \frac{\partial^2 \psi}{\partial x^2} + \frac{\partial^2 \psi}{\partial y^2} = 0 \end{cases} \quad (3)$$

$$\begin{cases} \bar{u}_x \frac{\partial \bar{u}_x}{\partial x} + \bar{u}_z \frac{\partial \bar{u}_x}{\partial z} + \frac{1}{\rho} \frac{\partial \bar{p}}{\partial x} = \nu \cdot (\frac{\partial^2 \bar{u}_x}{\partial x^2} + \frac{\partial^2 \bar{u}_x}{\partial z^2}) - (\frac{\partial \bar{u}_{xI}{}^2}{\partial x} + \frac{\partial \bar{u}_{xI} \bar{u}_{zI}}{\partial z}) \\ \bar{u}_x \frac{\partial \bar{u}_z}{\partial x} + \bar{u}_z \frac{\partial \bar{u}_z}{\partial z} + \frac{1}{\rho} \frac{\partial \bar{p}}{\partial z} = \nu \cdot (\frac{\partial^2 \bar{u}_z}{\partial x^2} + \frac{\partial^2 \bar{u}_z}{\partial z^2}) - (\frac{\partial \bar{u}_{zI}{}^2}{\partial z} + \frac{\partial \bar{u}_{xI} \bar{u}_{zI}}{\partial x}) \\ \frac{\partial \bar{u}_x}{\partial x} + \frac{\partial \bar{u}_z}{\partial z} = 0 \end{cases} \quad (5)$$

$$\begin{cases} \frac{\partial u_x}{\partial x} = O\left(\frac{U}{L}\right) \ ; \ \frac{\partial u_z}{\partial z} = O\left(\frac{W}{\delta}\right) = O\left(\frac{U\xi}{L}\right) \ ; \ u_x \frac{\partial u_x}{\partial x} = O\left(\frac{U^2}{L}\right) \ ; \ \frac{\partial u_x}{\partial t} = O\left(\frac{U}{T}\right) = O\left(\frac{U^2}{L}\right) \ ; \\ u_z \frac{\partial u_x}{\partial z} = O\left(W \frac{U}{\delta}\right) = O\left(\frac{U\delta}{L} \cdot \frac{U}{\delta}\right) = O\left(\frac{U^2}{L}\right) \ ; \ \nu \frac{\partial^2 u_x}{\partial x^2} = O\left(\frac{\nu \cdot U}{L^2}\right) = O\left(\frac{1}{\frac{UL}{\nu}} \cdot \frac{U^2}{L}\right) = O\left(\frac{1}{Re \frac{U^2}{L}}();\right) \\ \nu \frac{\partial^2 u_x}{\partial z^2} = O\left(\frac{1}{\xi^2 \cdot Re \frac{U^2}{L}}() \frac{\delta}{L} \frac{1}{\sqrt{Re}}\right) \end{cases} \quad (6)$$

$$\begin{cases} \frac{\partial u_z}{\partial t} = O\left(\frac{W}{T}\right) = O\left(\frac{1}{\sqrt{\mathrm{Re}}} \cdot \frac{U^2}{L}\right); u_x \frac{\partial u_z}{\partial x} = O\left(W \frac{U}{L}\right) = O\left(\frac{1}{\sqrt{\mathrm{Re}}} \cdot \frac{U^2}{L}\right); \\ u_z \frac{\partial u_z}{\partial z} = O\left(\frac{W^2}{\delta}\right) = O\left(\frac{1}{\sqrt{\mathrm{Re}}} \cdot \frac{U^2}{L}\right); \nu \frac{\partial^2 u_z}{\partial x^2} = O\left(\frac{\nu \cdot W}{L^2}\right) = O\left(\frac{1}{\mathrm{Re}\sqrt{\mathrm{Re}}} \cdot \frac{U^2}{L}\right); \\ \nu \frac{\partial^2 u_z}{\partial z^2} = O\left(\frac{\nu \cdot W}{\delta^2}\right) = O\left(\frac{1}{\xi^2 \cdot \mathrm{Re}\sqrt{\mathrm{Re}}} \cdot \frac{U^2}{L}\right); \end{cases} \quad (7)$$

$$\begin{cases} P_0 = P_{x=x_0} + (\frac{P_{x=x_1} - P_{x=x_0}}{x_1 - x_0}) \cdot (x - x_0) = P_{x=x_0} + (\frac{P_{x=x_1} - P_{x=x_0}}{x_1 - x_0}) \cdot (\vartheta_1 + \vartheta_2) \cdot (t - t_0) \\ P_4 = P_{x=x_4} + (\frac{P_{x=x_5} - P_{x=x_4}}{x_5 - x_4}) \cdot (x - x_4) = P_{x=x_4} + (\frac{P_{x=x_5} - P_{x=x_4}}{x_5 - x_4}) \cdot (\vartheta_1 + \vartheta_2) \cdot (t - t_4) \\ P_8 = P_{x=x_8} + (\frac{P_{x=x_9} - P_{x=x_8}}{x_9 - x_8}) \cdot (x - x_8) = P_{x=x_8} + (\frac{P_{x=x_9} - P_{x=x_8}}{x_9 - x_8}) \cdot (\vartheta_1 + \vartheta_2) \cdot (t - t_8) \\ \vdots \\ P_{n-1} = P_{x=x_{n-1}} + (\frac{P_{x=x_n} - P_{x=x_{n-1}}}{x_n - x_{n-1}}) \cdot (x - x_{n-1}) = P_{x=x_{n-1}} + (\frac{P_{x=x_n} - P_{x=x_{n-1}}}{x_n - x_{n-1}}) \cdot (\vartheta_1 + \vartheta_2) \cdot (t - t_{n-1}) \end{cases} \quad (12)$$

$$\begin{cases} P_1 = P_{x=x_1} + \frac{1}{2}\cdot(P_A - P_{x=x_1})\cdot(1 - cos(\frac{2\pi}{\lambda_1}\cdot(x - x_1))) = P_{x=x_1} + (P_A - P_{x=x_1})\cdot sin^2(\frac{\pi}{\lambda_1}\cdot(x - x_1)) = \\ = P_{x=x_1} + (P_A - P_{x=x_1})\cdot sin^2(\frac{\pi}{\lambda_1}\cdot(\vartheta_1 + \vartheta_2)\cdot(t - t_1)) \\ P_2 = \frac{1}{2}\cdot(P_A + P_B) + \frac{1}{2}\cdot(P_A - P_B)\cdot cos(\frac{2\pi}{\lambda_2}\cdot(x - x_2)) = \\ = \frac{1}{2}\cdot(P_A + P_B) + \frac{1}{2}\cdot(P_A - P_B)\cdot cos(\frac{2\pi}{\lambda_2}\cdot(\vartheta_1 + \vartheta_2)\cdot(t - t_2)) \\ P_3 = P_{x=x_4} - \frac{1}{2}\cdot(P_{x=x_4} - P_B)\cdot(1 - cos(\frac{2\pi}{\lambda_3}\cdot(x - x_3 + \frac{\lambda_3}{2}))) = \\ = P_{x=x_4} - \frac{1}{2}\cdot(P_{x=x_4} - P_B)\cdot(1 - cos(\frac{2\pi}{\lambda_3}\cdot((\vartheta_1 + \vartheta_2)\cdot(t - t_3) + \frac{\lambda_3}{2}))) \\ \vdots \\ P_{n-4} = P_{x=x_{n-4}} - \frac{1}{2}\cdot(P_{x=x_{n-4}} - P_{Bn})\cdot(1 - cos(\frac{2\pi}{\lambda_{n-4}}\cdot(x - x_{n-4}))) = \\ = P_{x=x_{n-4}} - \frac{1}{2}\cdot(P_{x=x_{n-4}} - P_{Bn})\cdot(1 - cos(\frac{2\pi}{\lambda_{n-4}}\cdot(\vartheta_1 + \vartheta_2)\cdot(t - t_{n-4}))) \\ P_{n-3} = \frac{1}{2}\cdot(P_{An} + P_{Bn}) - \frac{1}{2}\cdot(P_{An} - P_{Bn})\cdot cos(\frac{2\pi}{\lambda_{n-3}}\cdot(x - x_{n-3})) = \\ = \frac{1}{2}\cdot(P_{An} + P_{Bn}) - \frac{1}{2}\cdot(P_{An} - P_{Bn})\cdot cos(\frac{2\pi}{\lambda_{n-3}}\cdot(\vartheta_1 + \vartheta_2)\cdot(t - t_{n-3})) \\ P_{n-2} = P_{x=x_{n-1}} - \frac{1}{2}\cdot(P_{x=x_{n-1}} - P_{An})\cdot(1 - cos(\frac{2\pi}{\lambda_{n-2}}\cdot(x - x_{n-2} + \frac{\lambda_{n-2}}{2}))) = \\ = P_{x=x_{n-1}} - \frac{1}{2}\cdot(P_{x=x_{n-1}} - P_{An})\cdot(1 - cos(\frac{2\pi}{\lambda_{n-2}}\cdot((\vartheta_1 + \vartheta_2)\cdot(t - t_{n-2}) + \frac{\lambda_{n-2}}{2}))) \end{cases} \quad (13)$$

$$\begin{cases} \Delta P_{1y} = k_1^{high-speed}\cdot C_{p1y}\cdot\rho\cdot\frac{{\vartheta_1}^2}{2\cdot 3,6^2} \\ C_{p1y} = \frac{8}{\left(y - \frac{A_2}{2} + 2,10\right)^2} \\ \Delta P_{1z} = k_1^{high-speed}\cdot C_{p1z}\cdot\rho\cdot\frac{{\vartheta_1}^2}{2\cdot 3,6^2} \\ C_{p1z} = \frac{8,5}{(z - 1,9)^2} + 0,1 \end{cases} \quad (14)$$